International Journal of Engineering and Technology
Vol. 9, No. 1, 2024, pp. 09-25

www.ijet.ielas.org
ISSN: 2545-417X

Integrated Experimental and Simulation Investigation of Breakdown Voltage Characteristics Across Electrode Configurations in SF6 Circuit Breakers

Bo Guan[a], Qi Yu[a], Qingpeng Yuan[b], Shiwen Chen[b], Laiiln Chen[a], Su Guo[a], Peilong Zhu[c*]
[a] Xiangshan Research Institute, Ningbo University of Technology, Ningbo, 315799, China
[b] Lotus cars, Ningbo, 315336, China
[c] Naisen Electric, Ningbo, 315712, China
Email: peilongz@126.com

Received: 2024-02-22 Accepted: 2024-05-20 Published online: 2024-08-28

Abstract

This study investigates the breakdown voltage characteristics in SF6 circuit breakers, employing a novel approach that integrates both experimental investigations and finite element simulations. Utilizing a sphere-sphere electrode configuration, we meticulously measured the relationship between breakdown voltage and electrode gap distances ranging from 1 cm to 4.5 cm. Subsequent simulations, conducted using COMSOL Multiphysics, mirrored the experimental setup to validate the model's accuracy through a comparison of the breakdown voltage - electrode gap distance curves. The simulation results not only aligned closely with the experimental data but also allowed the extraction of detailed electric field strength, electric potential contours, and electric current flow curves at the breakdown voltage for gap distances extending from 1 to 4.5 cm. Extending the analysis, the study explored the electric field and potential distribution at a constant voltage of 72.5kV for gap distances between 1 to 10 cm, identifying the maximum electric field strength. A comprehensive comparison of five different electrode configurations (sphere-sphere, sphere-rod, sphere-plane, rod-plane, rod-rod) at 72.5kV and a gap distance of 1.84 cm underscored the significant influence of electrode geometry on the breakdown process. Moreover, the research contrasts the breakdown voltage in SF6 with that in air, emphasizing SF6's superior insulating properties. This investigation not only elucidates the intricate dynamics of electrical breakdown in SF6 circuit breakers but also contributes valuable insights into the optimal electrode configurations and the potential for alternative insulating gases, steering future advancements in high-voltage circuit breaker technology.

Keywords: SF6 circuit breaker, Breakdown voltage, Electrode configurations, COMSOL simulation, Electrical insulation.

1. Introduction

Insulation serves multiple critical functions in high-voltage devices, providing not only electrical isolation but also aiding in cooling and mechanical support, while

simultaneously possessing the capability to withstand high breakdown voltages. SF6 gas is widely recognized for its exceptional insulating and arc-quenching properties, making it a material of choice for use in various electrical switchgear applications, including circuit breakers and gas-insulated switchgear (GIS) [1-3]. With the increasing reliance on ultra-high-voltage direct current (UHVDC) systems in the architecture of modern power grids, there has been a heightened focus on the development of DC gas-insulated equipment [4,5]. In the realm of high-voltage technology, dielectric breakdown is a primary concern, often triggered by overvoltages caused by sparks during switching operations or due to lightning strikes.

The insulating characteristics of dielectric materials, particularly gaseous dielectrics, are garnering considerable attention due to their pivotal role in high-voltage equipment operation. Research efforts are increasingly focused on determining the precise breakdown voltage of SF6 gas across a variety of electrode configurations. These configurations are selected to generate both homogeneous and non-homogeneous electric fields, which are essential for in-depth studies of SF6 gas breakdown characteristics under different conditions. The choice of electrode configuration has been shown to significantly affect discharge behaviors and breakdown voltage levels [6]-[10].

Kyu Kim et al. [6] delved into the breakdown mechanisms of heated gases, examining the critical electric field as a dependent variable of both temperature and pressure. A Srikant [8] carried out simulations to ascertain the breakdown voltage of SF6 gas within a sphere-sphere electrode arrangement, varying the inter-electrode gap distances. It has been elucidated that the maximum electric field intensity is influenced not solely by the electrode geometry but also by an array of factors including the gap distance, applied voltage, and the environmental conditions of temperature and pressure [11],[12]. Furthermore, a collective study [13] employed various gap distances to empirically determine the breakdown voltage of SF6 gas, utilizing a node tank SF6 gas circuit breaker to analyze the patterns of abnormal electrical discharges.

Various researchers have undertaken comparative analyses of theoretical Breakdown Voltage (BDV) with empirical data and MATLAB simulations for SF6 gas, considering different electrode dimensions and spacings. Findings indicate that an increase in the gap between spherical electrodes results in a corresponding rise in both the breakdown voltage and the electric field strength, with the latter inversely related to the sphere's radius [14]. However, these studies often omitted a discussion on the dielectric breakdown mechanisms of SF6 gas.

Additionally, the quest for alternative arc-quenching and insulating materials has prompted comparative studies of SF6's dielectric breakdown performance against other gases, such as N2 [14]-[16], CF4 [17], and CO2 [17]-[19]. Despite these efforts, there

remains a gap in the literature concerning the behavior of SF6 breakdown at varying electrode gaps and under conditions of non-homogeneous electric stress. This paper aims to address these gaps by providing a comprehensive analysis of the breakdown characteristics of SF6 across different electrode configurations and gap distances, contributing to the broader understanding of GIS insulation performance.

Building on the foundation of existing research, this paper seeks to bridge the gaps identified in the current body of knowledge regarding the dielectric breakdown of SF6 gas in various high-voltage applications. While previous studies have provided valuable insights into the breakdown voltages across different electrode configurations and the comparative dielectric strengths of various insulating media, there remains a need for a more detailed understanding of SF6 breakdown phenomena, especially in non-homogeneous electric fields and at varying electrode gaps.

This study aims to extend the current understanding by conducting a series of experiments and simulations to examine the breakdown characteristics of SF6 with a particular focus on the influence of electrode geometry and gap distances. Through experimental setups and COMSOL Multiphysics simulations, asserting the superiority of SF6 as an insulator compared to air.

This investigation is poised at the intersection of experimental precision and advanced simulation capabilities, targeting a dual-faceted analysis of breakdown voltage phenomena within SF6 circuit breakers. By adopting a sphere-sphere electrode configuration, this study meticulously quantifies the breakdown voltage across a range of electrode gap distances, thereby laying the groundwork for a robust comparison with simulated models. The utilization of COMSOL Multiphysics for these simulations not only reinforces the experimental findings but also enhances our understanding of the electric field, potential and current flow characteristics under conditions leading to electrical breakdown.

The analysis is further extended to encompass an array of electrode configurations under a uniform high voltage, revealing the critical role of electrode geometry in the breakdown process. In conjunction with this, the comparison of breakdown voltages in SF6 and air provides a stark illustration of the superior insulation capacity offered by SF6—information that is indispensable for the design and optimization of high-voltage switchgear.

As we delve into the intricate mechanisms of electrical breakdown, the insights gleaned from this study are anticipated to pave the way for innovations in circuit breaker technology, potentially catalyzing the development of new insulating materials. The final segment of this introduction sets the stage for a detailed exposition of the methods and findings that follow, ultimately guiding the discourse towards enhancing the operational efficiency and safety of high-voltage electrical systems.

2. Methodology

2.1. Experiment

In the experimental setup illustrated in Figure 1a, a sphere-sphere electrode configuration was placed within a sealed chamber filled with SF6 gas, sourced from an SF6 gas pump. This configuration was then connected to an AC/DC generator to facilitate the application of electrical potential across the electrodes. The differential in electric potential between the two electrodes was meticulously recorded using a voltage probe. The testing apparatus, depicted in Figure 1b, was acquired from Hezhong Electric Equipment, capable of generating voltages up to 150 kV at power frequency. For this experiment, the SF6 gas was maintained at a pressure of 0.15 MPa. Both sphere electrodes, utilized in the setup, boasted a diameter of 4 cm, ensuring uniformity in the experimental conditions.

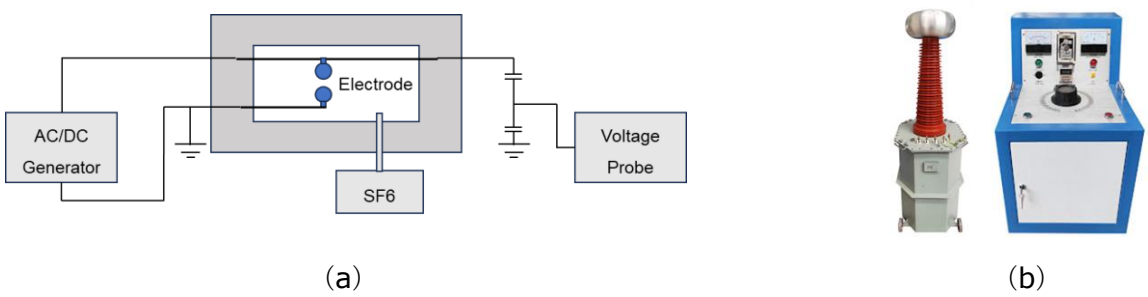

(a) (b)

Figure 1 (a). A schematic drawing of the schematic experiment setup. (b) Test machine.

2.2. Simulation

To complement the experimental investigation, a detailed finite element simulation was conducted using COMSOL Multiphysics software, aimed at replicating the electric breakdown scenarios observed in the SF6 circuit breakers under study. This simulation methodology was meticulously designed to mirror the experimental setup, thereby facilitating a direct comparison between the simulated and experimental results.

The simulation began with the creation of a two-dimensional model representing the sphere-sphere electrode configuration within a chamber filled with SF6 gas, as shown in Figure 2a. The geometrical dimensions, including the 4 cm diameter of the sphere electrodes and the variable gap distances ranging from 1 cm to 4.5 cm, were precisely replicated as per the experimental design. The geometry domain was discretized using a triangular mesh to ensure detailed and accurate representation of the geometry for the finite element analysis.

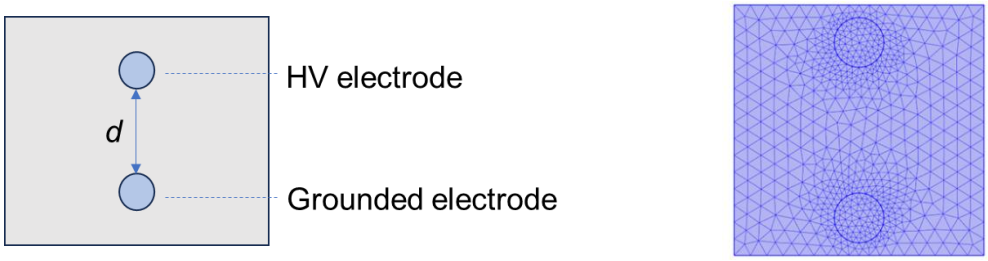

Figure 2 (a). The two-dimensional geometry model created in COMSOL Multiphysics; (b) The finite element model.

To thoroughly investigate the impact of electrode configurations on electric breakdown, the simulation extended to include various electrode setups: sphere-sphere, sphere-rod, sphere-plane, rod-plane, and rod-rod, as shown in Figure 3. These configurations were simulated at a fixed gap distance and voltage to determine their influence on the breakdown mechanism. This comprehensive approach allowed for an in-depth analysis of how different electrode geometries affect the initiation and propagation of electric breakdown in SF6.

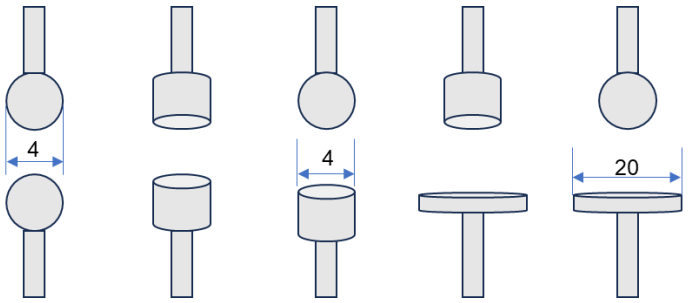

Figure 3. A schematic drawing of different electrode configurations: sphere-sphere, sphere-rod, sphere-plane, rod-plane, and rod-rod.

Electrical properties of the materials were crucial for accurate simulation. Specifically, the relative permittivity (dielectric constant) of SF6 was set to 1.002, and for air, it was set at 1, with the breakdown electric field strength in SF6 considered to be 89kV/cm, and in air, 30kV/cm. These parameters underscore the superior insulating properties of SF6, even with a relative permittivity nearly identical to air.

The AC/DC module of COMSOL Multiphysics was utilized to simulate the electric field distribution, potential difference, and current flow within the setup for the range of electrode gap distances and configurations. Incremental application of potential difference across the electrodes was performed until electric breakdown was observed in the model, facilitating the extraction of breakdown voltage values for comparison with experimental data.

Additionally, the simulation's scope included analyzing electric field strength, potential contours, and current flow paths at critical points leading to breakdown, especially at a constant voltage of 72.5kV and varying electrode gap distances up to 10 cm.

Integrating electric field, potential, and current flow data from the simulations, the study offered a comprehensive understanding of factors influencing electric breakdown in SF6 circuit breakers.

3. Results

The primary objective of our research was to compare the breakdown voltage in an SF6 circuit breaker as a function of the electrode gap distance, using both experimental methods and finite element simulation. The experimentally measured and simulated breakdown voltages across electrode gap distances ranging from 1 cm to 4.5 cm are presented in Figure 4.

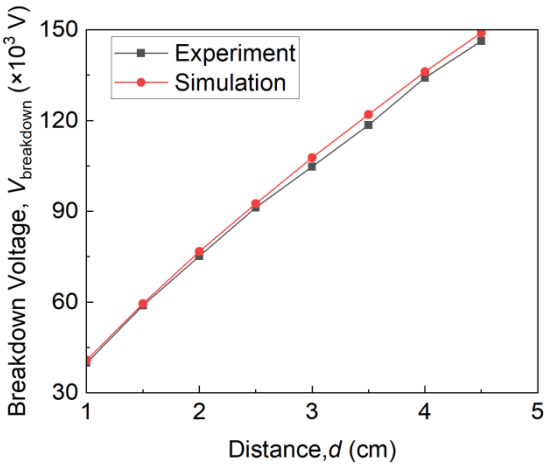

Figure 4. The breakdown voltage of sphere-sphere configuration in SF6 circuit breaker from experiment and simulation.

The experimental data delineate a clear linear correlation between the breakdown voltage and the electrode gap distance, which was anticipated based on the known behavior of dielectrics. The breakdown voltage increases from 39.8 kV at a 1 cm gap distance to about 146 kV at a 4.5 cm gap distance. This trend is in line with the classical Paschen's Law, which describes the breakdown voltage as a function of the product of pressure and gap distance in homogeneous electric fields.

Parallel to the experimental measurements, the simulations conducted within COMSOL Multiphysics exhibited a remarkably similar trend, closely shadowing the experimental results. The simulation data points of the breakdown voltage increases

from 40.8 kV at a 1 cm gap distance to about 149 kV at a 4.5 cm gap distance, showcasing only slight deviations within the margin of experimental error. The close agreement between the experimental and simulated values suggests the validity and accuracy of the simulation model, affirming its potential as a predictive tool for electrical breakdown in SF6 circuit breakers, providing a solid foundation for further research and development in this field.The linear relationship observed in the results confirms the expectation that the breakdown voltage is proportional to the distance in the range studied, reinforcing the theory that the electric field distribution between sphere-sphere electrode configurations remains uniform as the gap increases.

Figure 5 presents a series of simulations that illustrate the electric field strength, potential distribution, and current flow within a sphere-sphere electrode setup in an SF6 circuit breaker environment at varying gap distances. Panels (a) through (f) represent the gap distances at 1, 1.5, 2, 2.5, 3.5, and 4.5 cm, respectively.

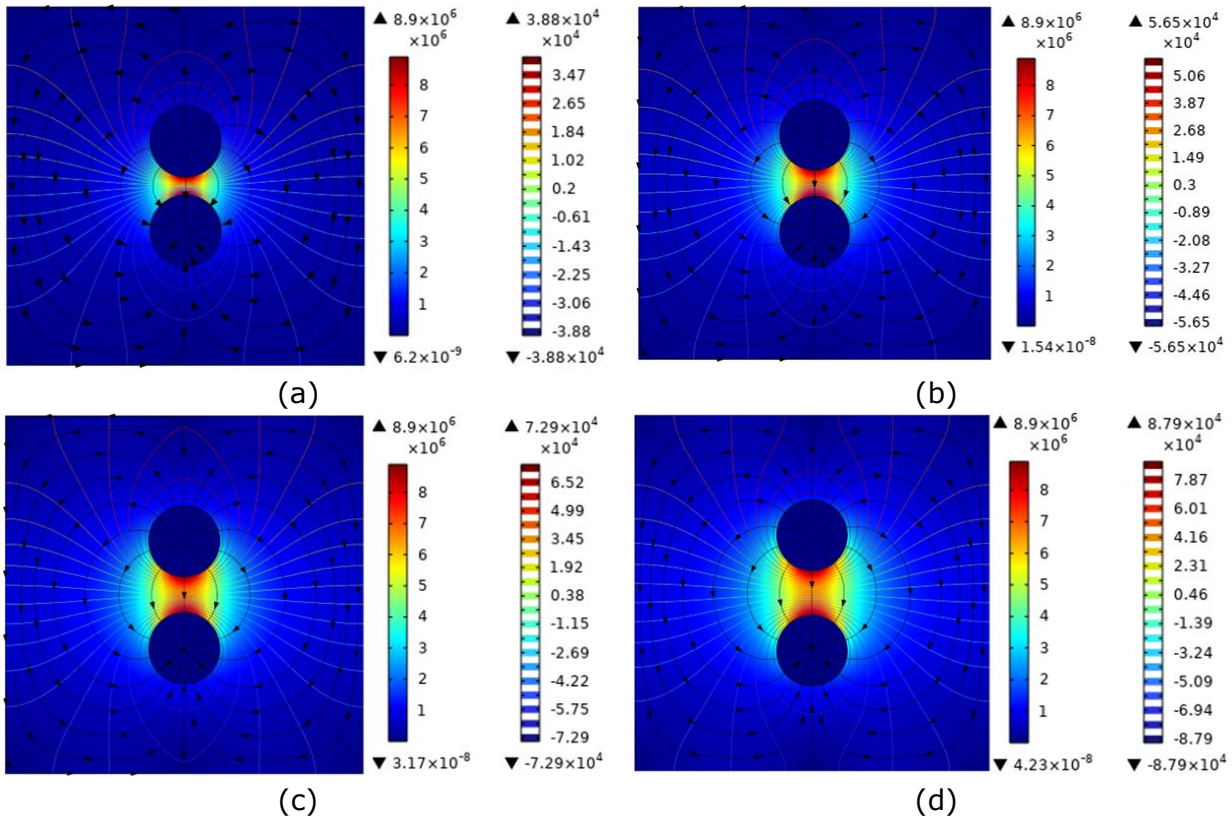

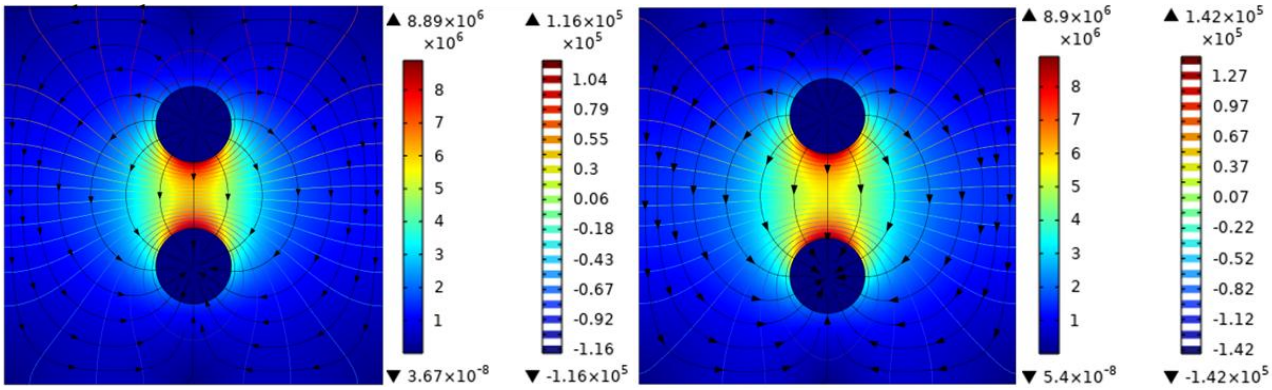

(e) (f)

Figure 5. The electric field strength, potential distribution, and current flow within a sphere-sphere electrode setup in an SF6 circuit breaker environment at varying gap distances. (a) 1 cm; (b) 1.5 cm; (c) 2 cm; (d) 2.5 cm; (e) 3.5 cm; (a) 4.5 cm.

At the smallest gap distance of 1 cm, as shown in Figure 5a, the electric field strength is observed to be highly concentrated between the electrodes, with a rapid decrease in strength moving outward from the gap's center. The potential distribution appears relatively uniform across the gap, and the current flow is directed predominantly between the two electrodes with minimal dispersion.

As the gap distance increases to 1.5 cm and 2 cm, depicted in Figure 5 (b) and (c), the electric field strength remains focused between the electrodes but begins to show a wider spread across the gap. The potential distribution starts to exhibit a more pronounced gradient from one electrode to the other, and the current flow patterns become slightly more dispersed.

Figure 5d at 2.5 cm gap distance reveals further spreading in the electric field strength with less intensity directly between the electrodes compared to shorter gap distances. The potential distribution gradient becomes steeper, indicating a change in the voltage drop across the gap. Additionally, current flow lines illustrate increased spreading with distance.

At a gap distance of 3.5 cm, shown in Figure 5e, the electric field distribution is wider, and the intensity between the electrodes is reduced compared to smaller gaps. The potential now shows a more significant gradient, and the current flow lines are more distributed across the gap, suggesting a shift in the overall field behavior.

Finally, at the largest gap distance of 4.5 cm in Figure 5f, the electric field strength is more evenly distributed throughout the space between the electrodes, with a much gentler gradient in potential distribution. The current flow lines are more widely spread across the gap, indicating the influence of the increased gap on the electrical characteristics.

The results indicate that as the gap distance increases, there is a notable transition in the electric field strength from a highly concentrated state to a more evenly distributed state. The potential distribution becomes less uniform, and the current flow patterns become more dispersed. These changes are indicative of the influence that the gap distance has on the behavior of electric breakdown phenomena within the electrode setup, providing valuable insights into the design and optimization of SF6 circuit breakers.

4. Discussion

4.1 Electric field strength with gap distance

Figure 6 provides a visualization of the electric field intensity, potential distribution, and current flow patterns at a fixed voltage of 72.5kV for different electrode gap distances in an SF6 circuit breaker model. The six panels, labeled (a) to (f), correspond to gap distances of 1, 3, 5, 7, 9, and 10 cm, respectively.

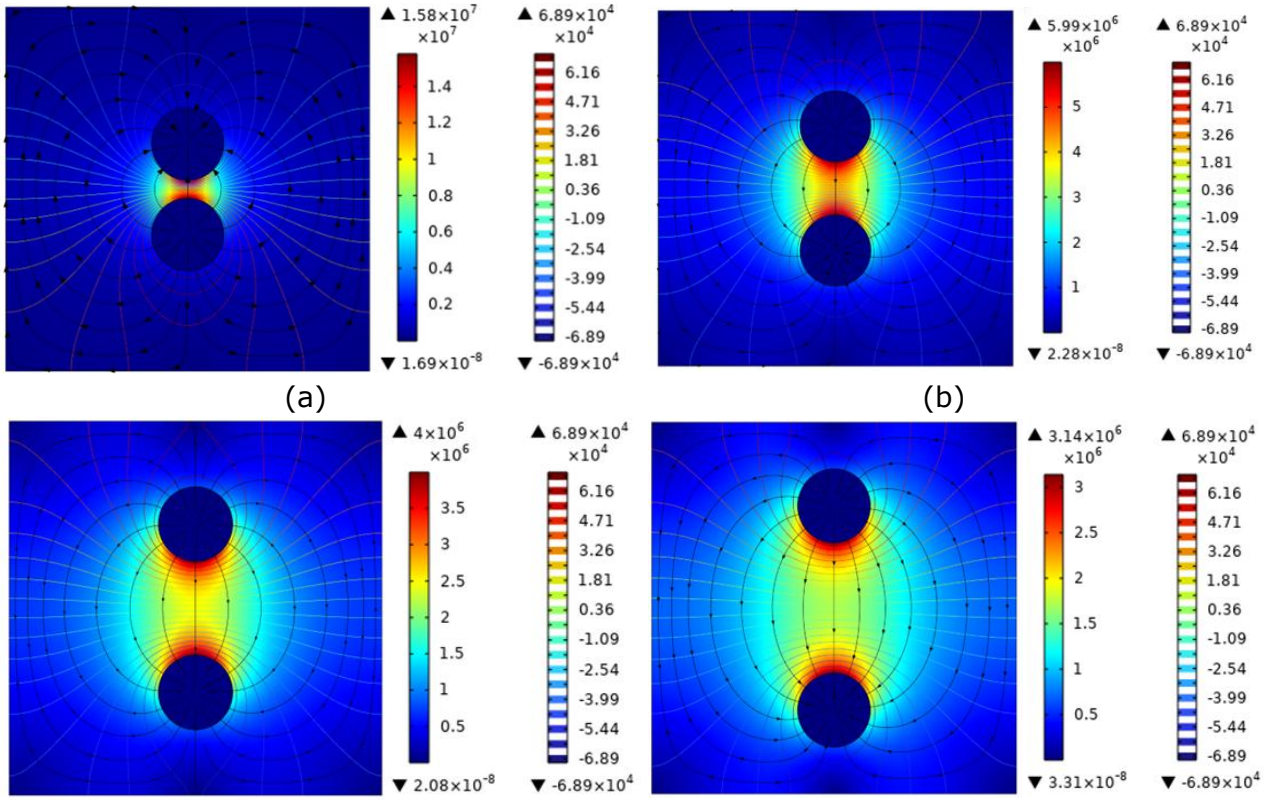

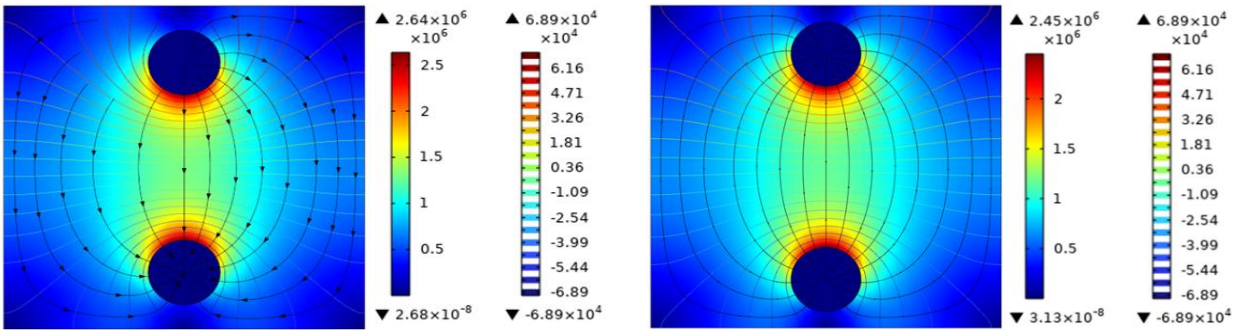

Figure 6. The electric field strength, potential distribution, and current flow within a sphere-sphere electrode setup at a fixed voltage of 72.5kV for different electrode gap distances in an SF6 circuit breaker model. (a) 1 cm; (b) 3 cm; (c) 5 cm; (d) 7 cm; (e) 9 cm; (a) 10 cm;

Figure 6a displays the scenario at the smallest gap distance of 1 cm. Here, the electric field shows a peak concentration in the narrow space between the electrodes, with the potential distribution indicating a steep gradient and the current flow lines densely packed, signifying a strong, localized electric field conducive to breakdown.

As the gap distance expands to 3 cm and 5 cm in Figure 6b and Figure 6c, the electric field intensity starts to spread out more evenly between the electrodes, albeit still maintaining a higher concentration at the center of the gap. The potential distribution becomes less steep compared to the 1 cm gap, and current flow lines show a broader distribution across the gap, suggesting a more distributed electric field environment.

At larger gap distances of 7 cm and 9 cm, shown in Figure 6d and Figure 6e, the electric field intensity further decreases in concentration between the electrodes. The potential gradient flattens progressively, and the current flow lines extend over a wider area, indicating a reduction in the likelihood of localized electric breakdown.

Figure 6f illustrates the conditions at a gap distance of 10 cm. Here, the electric field intensity is the most distributed, with the lowest concentration at the midpoint between the electrodes. The potential gradient is the flattest among all the scenarios, and the current flow lines are the most dispersed, suggesting the lowest electric stress and hence the lowest propensity for electric breakdown.

Overall, the results demonstrate a clear trend: as the gap distance increases, the electric field intensity becomes more evenly distributed, the potential gradient lessens, and the current flow lines indicate a wider area of influence

Figure 7 illustrates the variation in maximum electric field strength as the electrode gap distance is increased from 1 to 10 cm. The data is extracted from Figure

6 and captures a distinct trend where the maximum electric field strength sharply declines as the distance between the electrodes is widened.

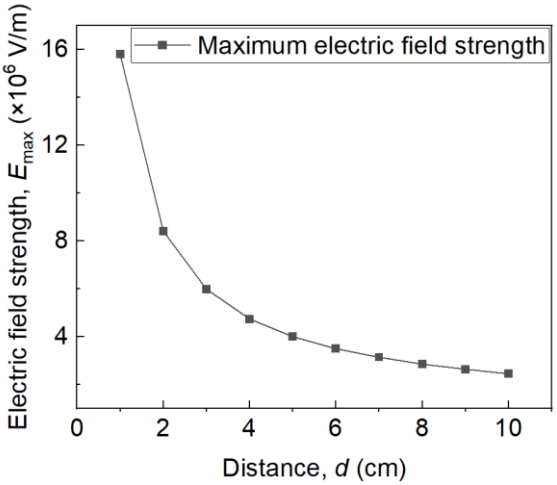

Figure 7. The variation in maximum electric field strength as the electrode gap distance increased from 1 to 10 cm.

At the outset, with the electrodes at the smallest separation of 1 cm, the maximum electric field strength is observed to be at its peak, approximately 158kV/cm. This high intensity is indicative of a strong, concentrated electric field expected in close-proximity electrode arrangements.

As the gap distance increases to 2 cm, there is a significant drop in the electric field strength, indicating a rapid decrease in the electric stress between the electrodes. This initial reduction in electric field strength demonstrates the non-linear sensitivity of electric field concentration to gap spacing in the initial stages.

Progressing further, the decline in electric field strength continues, but at a more gradual rate. The plot shows a discernible leveling off as the gap distance extends beyond 4 cm, trending towards a more stable value around 25 kV/cm as the distance approaches 10 cm. This gradual decrease suggests a tapering influence of distance on field strength for larger electrode separations.

The curve's profile provides valuable insights into the dielectric strength of SF6 and its ability to withstand electric fields over varying distances, since the critical electric breakdown of the electric field strength is 89 kV/cm. The decreasing trend of the electric field strength with increasing gap distance is consistent with the theoretical understanding that the potential for dielectric breakdown reduces as the electrode separation grows, up to a point where the field becomes insufficient to initiate a breakdown.

4.2 Electric field strength with different configuration

Figure 8 depicts the simulation results for the electric field intensity, potential distribution, and current flow patterns at a critical voltage of 72.5kV and a gap distance of 1.84 cm, which has been identified as the critical distance for electric breakdown in a sphere-sphere electrode configuration within an SF6 environment.

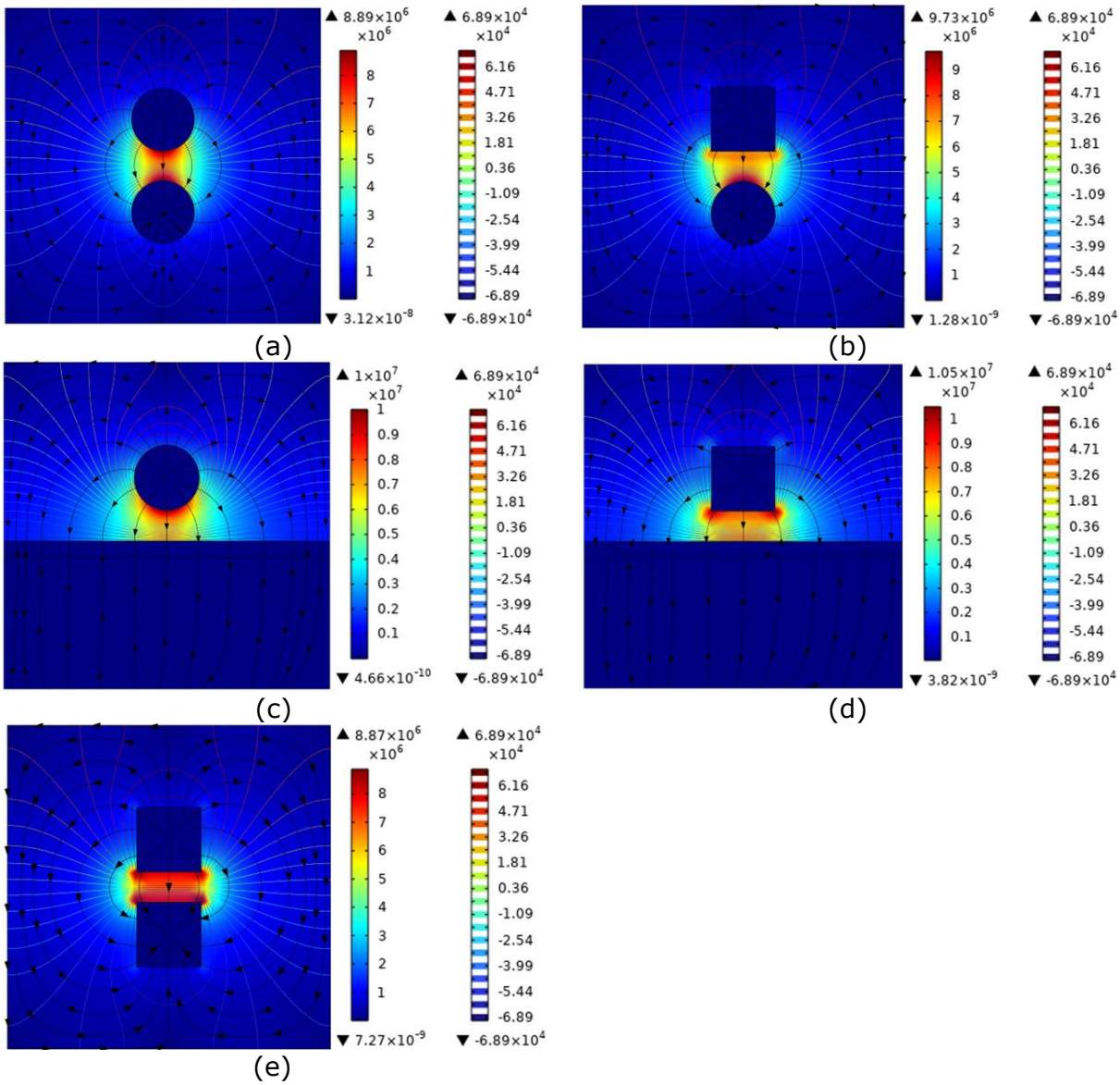

Figure 8. Simulation results for the electric field intensity, potential distribution, and current flow patterns at a critical voltage of 72.5kV and a gap distance of 1.84 cm

Figure 8a demonstrates the sphere-sphere configuration, where the maximum electric field strength is observed at 89kV/cm. The electric field is symmetrically

distributed between the spheres, with a clear high-intensity region connecting the two electrodes. The potential contours are evenly spaced, and the current flow is centralized between the electrodes, indicating a concentrated breakdown path.

The sphere-rod configuration, shown in Figure 8b, exhibits a higher maximum electric field strength of 97.3 kV/cm. The field is intensified at the rod tip, illustrating the effect of geometry on field enhancement. The potential distribution is more concentrated around the rod, and the current flow lines are more focused towards the rod's tip, suggesting a higher propensity for electric breakdown at this point.

In Figure 8c, the sphere-plane configuration, the electric field strength is slightly lower than the sphere-sphere case, at 88.7kV/cm. The field disperses across the plane's surface, with the potential lines indicating a more gradual voltage drop and the current flow spreading out over a larger area, reducing the concentration of electrical stress.

The rod-plane configuration depicted in Figure 8d shows the maximum electric field strength of 105 kV/cm, the highest among the configurations. This is attributed to the pronounced field concentration at the rod's tip, which is in close proximity to the plane, creating a condition highly conducive to breakdown.

Finally, the rod-rod configuration Figure 8e has a maximum electric field strength of 100 kV/cm. Similar to the sphere-sphere setup, the electric field is symmetrically concentrated between the rods, but with a slightly higher intensity due to the shape of the electrodes, highlighting the rod's geometry's influence on the field strength.

A comparative analysis across five different electrode configurations: sphere-sphere, sphere-rod, sphere-plane rod-plane and rod-rod, with corresponding maximum electric field strengths was summarized in Table 1.

Table 1. The configurations and their corresponding maximum electric field strength

Configuration	Sphere-sphere	Sphere-rod	Sphere-plane	Rod-plane	Rod-rod
Maximum Electric Field Strength, E_{max} ($x10^6$V/m)	8.89	9.73	8.87	10.5	10.0

The results indicate that the maximum electric field strength varies significantly with the shape of the electrode configuration. Among the five configurations tested at the critical gap distance of 1.84cm under a voltage of 72.5kV in an SF6 environment,

the rod-plane configuration exhibits the highest maximum electric field strength at 105kV/cm. This suggests that the rod-plane configuration is the most prone to electric breakdown under these specific conditions due to the intense concentration of the electric field at the rod's tip.

Conversely, the configuration with the lowest maximum electric field strength is the sphere-plane at 88.7kV/cm, which is nearly the same as sphere-sphere configuration, indicating a more resistant behavior towards electric breakdown compared to the others.

4.3 Breakdown voltage with insulating gas

Figure 9 presents a comparative analysis of the breakdown voltage as a function of the electrode gap distance in two different gaseous environments: sulfur hexafluoride (SF6) and air. The breakdown voltage is plotted against the electrode gap distance ranging from 1 cm to 4.5 cm.

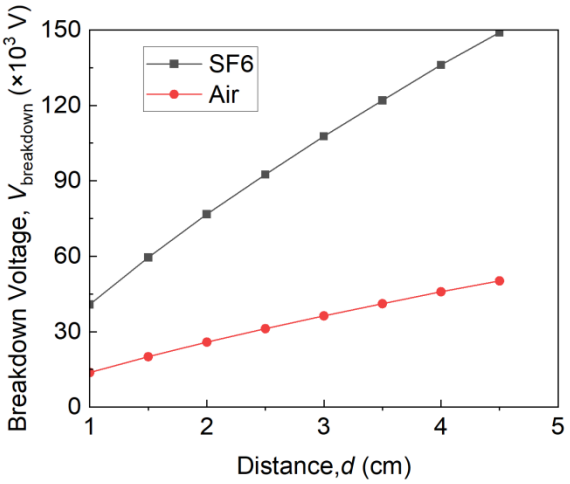

Figure 9. The breakdown voltage changes with the electrode gap distance in sulfur SF6 and air environment.

For SF6, the breakdown voltage increases linearly with the gap distance, starting from approximately 40.8 kV at a 1 cm gap and reaching up to 149 kV at a 4.5 cm gap. This trend reflects the robust insulating properties of SF6, which is widely recognized for its high dielectric strength and ability to prevent electrical discharges.

In contrast, the curve for air presents a much lower breakdown voltage, starting just above 13.8 kV at a 1 cm gap and increasing to about 50.2 kV at a 4.5 cm gap. The relatively flat slope of the curve for air suggests a marginal increase in breakdown voltage with the increase in gap distance, indicating the lesser insulating effectiveness of air compared to SF6.

The marked difference between the two curves underscores the superior dielectric strength of SF6 over air, demonstrating its effectiveness in insulating electrical components and preventing breakdown over a wide range of electrode gap distances. The data highlight SF6's critical role in high-voltage applications, where maintaining electrical integrity is of paramount importance.

4. Conclusion

The comprehensive study encompassing experimental analysis and finite element simulation has provided significant insights into the breakdown voltage characteristics of SF6 circuit breakers. Our investigation demonstrated a linear increase in breakdown voltage with electrode gap distance, confirming the expected behavior as per Paschen's Law. The remarkable congruence between experimental data and simulation results validates the accuracy of the finite element model in predicting electrical breakdown phenomena.

Further analysis revealed the critical impact of electrode configuration on electric field distribution, with the rod-plane configuration showing the highest electric field strength, thus the greatest susceptibility to breakdown at a critical distance of 1.84 cm. Conversely, the sphere-plane configuration exhibited the lowest electric field strength, suggesting enhanced resistance to breakdown under the tested conditions.

A key takeaway from our study is the pronounced superiority of SF6 over air as an insulating medium. SF6's robust dielectric properties significantly elevate the breakdown voltage, reinforcing its application in high-voltage circuit breakers. However, the influence of electrode geometry remains a decisive factor in the design and performance of these circuit breakers.

This research not only advances our understanding of electric breakdown in SF6-insulated systems but also emphasizes the need for careful consideration of electrode design to optimize the performance and reliability of high-voltage electrical infrastructure.

Acknowledgement

We would like to express our deepest gratitude to [Ningbo Science and Technology Plan Project] for their generous support through Grant No. [2023Z043]. This funding was pivotal in enabling us to carry out our research

References

[1]. T. Silkstone, "Sulpur Hexafluoride Emissions and its Affect on the Environment Sulphur Hexafluoride in the Environment October 2019 Thomas Silkstone," no. October, 2019.

[2]. N. A. M. Amin, M. T. Ishak, M. H. A. Hamid, and M. S. Abd Rahman, "Partial discharge investigation on palm oil using needle - plane electrode configuration and electric field distribution using ansys maxwell," Int. Conf. High Volt. Eng. Power Syst. ICHVEPS 2017 -Proceeding, vol. 2017-Janua, no. January 2018, pp. 440–445, 2017.

[3]. M. S. Laili and N. Yusof, "Modelling of Mathematical Equation for Determining Breakdown Voltage," pp. 3–7, 2013.

[4]. D. Kamthe and N. R. Bhasme, "Comparative analysis between Air Insulated and Gas Insulated Substation - A review," Int. J. Electr. Eng. Technol., vol. 9, no. 4, pp. 24–32, 2018.

[5]. E. Foruzan, A. A. S. Akmal, K. Niayesh, J. Lin, and D. D. Sharma, "Comparative study on various dielectric barriers and their effect on breakdown voltage," High Volt., vol. 3, no. 1, pp. 51–59, 2018.

[6]. A. Ayub, C. M. Invernizzi, G. Di Marcoberardino, P. Iora, and G. Manzolini, "Carbon dioxide mixtures as working fluid for high-temperature heat recovery: A thermodynamic comparison with transcritical organic rankine cycles," Energies, vol. 13, no. 15, 2020.

[7]. H. Kim, J. Chong, and K. Song, "Analysis of Dielectric Breakdown of Hot SF 6 Gas in a Gas Circuit Breaker," vol. 5, no. 2, pp. 264–269, 2010.

[8]. S.-Y. Woo, D.-H. Jeong, K.-B. Seo, and J.-H. Kim, "A Study on Dielectric Strength and Insulation Property of SF 6 /N 2 Mixtures for GIS ," J. Int. Counc. Electr. Eng., vol. 2, no. 1, pp.104–109, 2012.

[9]. M. Danikas, G. E. Vardakis, and R. Sarathi, "Some Factors Affecting the Breakdown Strength of Solid Dielectrics: A Short Review," Eng. Technol. Appl. Sci. Res., vol. 10, no. 2, pp. 5505–5511, 2020.

[10]. M. Koch, "Prediction of Breakdown Voltages in Novel Gases for High Voltage Insulation," no. July 1984, 2015.

[11]. D. A. Glushkov, A. I. Khalyasmaa, S. A. Dmitriev, and S. E. Kokin, "Electrical Strength Analysis of SF6 Gas Circuit Breaker Element," AASRI Procedia, vol. 7, pp. 57–61, 2014.

[12]. M. T. Ishak, N. Aqilah, M. Amin, M. Hayati, and A. Hamid, "Partial Discharge Investigation on Palm Oil Using Needle – Plane Electrode Configuration and Electric Field Distribution Using ANSYS Maxwell," no. October, 2017.

[13]. H.-K. Kim, J.-K. Chong, and K.-D. Song, "Analysis of Dielectric Breakdown of Hot SF 6 Gas in a Gas Circuit Breaker," 2010.

[14]. J. Lin, "Comparative study on various dielectric barriers and their effect on breakdown voltage barriers and their effect on breakdown voltage," 2018.
[15]. S. Woo et al., "A Study on Dielectric Strength and Insulation Property of SF 6 / N 2 Mixtures for GIS A Study on Dielectric Strength and Insulation Property of SF 6 / N 2 Mixtures for GIS," vol. 8972, 2014.
[16]. P. Control, "Measurement of air breakdown voltage and electric field using standard sphere gap method," 2011.
[17]. K. L. Ratnakar and B. R. Kamath, "Influence of Electrode Configuration on AC Breakdown Voltages," vol. IV, no. Vi, pp. 60–63, 2017.